

AD-A048 751

NAVAL RESEARCH LAB WASHINGTON D C  
REFLEX TETRODE WITH UNIDIRECTIONAL ION FLOW.(U)  
NOV 77 J A PASOUR, R A MAHAFFEY, J GOLDEN

F/G 9/1

UNCLASSIFIED

NRL-MR-3670

SBIE-AD-E000 073

NL

| 0f |

ADAO48 751



END

DATE  
FILMED

2 -78

DDC

12  
NW

NRL Memorandum Report 3670

AD A048751

## Reflex Tetrode with Unidirectional Ion Flow

J. A. PASOUR, R. A. MAHAFFEY, J. GOLDEN and C. A. KAPETANAKOS

*Experimental Plasma Physics Branch  
Plasma Physics Division*

November 1977

ade 000073



NAVAL RESEARCH LABORATORY  
Washington, D.C.

DDC  
RECEIVED  
JAN 19 1978  
B

AD No. 1  
DDC FILE COPY

Approved for public release; distribution unlimited.

SECURITY CLASSIFICATION OF THIS PAGE (When Data Entered)

REPORT DOCUMENTATION PAGE		READ INSTRUCTIONS BEFORE COMPLETING FORM
1. REPORT NUMBER NRL Memorandum Report 3670	2. GOVT ACCESSION NO.	3. RECIPIENT'S CATALOG NUMBER (9)
4. TITLE (and Subtitle) REFLEX TETRODE WITH UNIDIRECTIONAL ION FLOW.	5. TYPE OF REPORT & PERIOD COVERED Interim report on a continuing NRL problem.	
7. AUTHOR(s) J. A. Pasour, R. A. Mahaffey, J. Golden and C. A. Kapetanakis Jeffrey Golden Christos A. Kapetanakis	6. PERFORMING ORG. REPORT NUMBER	
8. PERFORMING ORGANIZATION NAME AND ADDRESS Naval Research Laboratory Washington, D. C. 20375	9. CONTRACT OR GRANT NUMBER(s)	
11. CONTROLLING OFFICE NAME AND ADDRESS Office of Naval Research Arlington, Virginia 22217	10. PROGRAM ELEMENT, PROJECT, TASK AREA & WORK UNIT NUMBERS NOTE: SITE SUPPLIED NRL Problem H02-28A NOTE Proj data 10/17/75	
14. MONITORING AGENCY NAME & ADDRESS (if different from Controlling Office) (12) 12p.	12. REPORT DATE November 1977 61153N	
	13. NUMBER OF PAGES 12	
	15. SECURITY CLASS. (of this report) UNCLASSIFIED	
16. DISTRIBUTION STATEMENT (of this Report) Approved for public release; distribution unlimited. (14) NRL-MR-3670		15a. DECLASSIFICATION/DOWNGRADING SCHEDULE DDC RECEIVED JAN 19 1978 B
17. DISTRIBUTION STATEMENT (of the abstract entered in Block 20, if different from Report) (16) RR01109 (17) RR0110941		
18. SUPPLEMENTARY NOTES †NRC Research Associate at Naval Research Laboratory This research was supported by the Office of Naval Research and the Department of Energy.		
19. KEY WORDS (Continue on reverse side if necessary and identify by block number) Intense ion sources (18) SBIE Reflex tetrode Reflex triode (19) AD-E000 073		
20. ABSTRACT (Continue on reverse side if necessary and identify by block number) Experimental results are reported which show that the backward directed (and unusable) ion current in a reflex triode can be almost completely suppressed by adding a second anode, made of aluminized mylar, 0.5 cm from the existing polyethylene anode. Proton generation efficiencies in excess of 50% have been obtained.		

DD FORM 1 JAN 73 1473

EDITION OF 1 NOV 65 IS OBSOLETE  
S/N 0102-014-6601

SECURITY CLASSIFICATION OF THIS PAGE (When Data Entered)

251 950

LB



## REFLEX TETRODE WITH UNIDIRECTIONAL ION FLOW

ACCESSION for		
NTIS	White Section	<input checked="" type="checkbox"/>
DOC	Buff Section	<input type="checkbox"/>
UNANNOUNCED		<input type="checkbox"/>
JUSTIFICATION _____		
BY _____		
DISTRIBUTION/AVAILABILITY CODES		
Dist.	AVAIL. and/or	SPECIAL
A		

During the last few years, remarkable progress has been made on the development of pulsed, high current ion sources.<sup>1-9</sup> Presently, pulsed ion sources are available<sup>1,3</sup> at power levels in excess of 0.2 terrawatts, and even higher power levels are anticipated in the near future. Among the various ion sources the reflex triode has several attractive features. For example, it can operate in the presence of a magnetic field and its ion current can be considerably higher than that predicted for bipolar flow. However, the reflex triode has the undesirable feature that about one half of the ion current flows toward the cathode of the device and thus is wasted. Therefore, under the best conditions, the optimum efficiency of an ordinary reflex triode cannot exceed 50%. For any practical device the efficiency is less than 30%.

In this letter we report results which demonstrate that by adding a second anode to an ordinary reflex triode the wasted ion current can be reduced to  $\leq 5\%$ , i.e.,  $\geq 95\%$  of the ion current propagates toward the virtual cathode and thus can be extracted out of the source and be utilized. So far, ion generation efficiencies in excess of 50% have been obtained.

The reflex tetrode configuration with double anode is illustrated schematically in Fig. 1a. A 5-cm diam. graphite cathode, maintained at ground potential, is located  $\sim 1.5$  cm from the first anode,  $A_1$ . This anode consists of a 6- $\mu\text{m}$ -thick aluminized mylar foil. The second anode,  $A_2$ , is placed  $\approx 0.5$  cm from  $A_1$  toward the virtual cathode and is made of a 13- $\mu\text{m}$ -thick polyethylene foil which

Note: Manuscript submitted November 30, 1977.

is the primary source of protons. The anodes are mounted on the edges of a 12.7 cm I.D. aluminum ring that is connected to the Seven Ohm Line (SOL) generator, which is operated in positive polarity. Typical peak output voltage of this generator is  $\sim 500$  kV with a pulse width of  $\sim 50$  nsec (FWHM). The experiments are performed with an axial magnetic field of  $\sim 5.6$  kG.

The motivation for using this double anode geometry was to obtain an electric potential profile in which protons from the anode plasma would be preferentially accelerated in the forward direction, i.e., toward the virtual cathode. In an ordinary reflex triode, the potential is more or less symmetric in the vicinity of the anode, so protons are emitted in both the forward and backward directions in approximately equal numbers. The addition of the second anode modifies the potential in such a way that most of the ions emitted at  $A_2$  are unable to reach  $A_1$ . Qualitatively, the potential profile of the double anode configuration is shown in Fig. 1b. The number of protons emitted from  $A_1$  toward the cathode K is small because, as has been observed in previous experiments,<sup>10</sup> aluminized mylar anodes are poor sources of protons.

The number of protons emitted in either direction is determined by nuclear activation techniques.<sup>11</sup> Thick graphite or boron nitride (BN) targets are placed  $\sim 7$  cm from  $A_2$  to measure the forward-directed number of protons. The number of back-directed protons is determined by measuring the activity induced in the graphite cathode and on BN or carbon targets placed around the cathode. In cases where the proton flux is intense enough to cause substantial target blow off, a 33% transparent screen is placed in front of the target to reduce the number of protons striking the target.

Since nuclear activation gives only the time integrated proton yield, the proton current is inferred from the total yield together with the duration

of the proton pulse. The duration of the proton pulse is assumed to be equal to the time interval from plasma formation until the diode voltage drops below the threshold for target activation (277 kV for the  $^{14}\text{N}(p,\gamma)^{15}\text{O}$  reaction on BN, 430 kV for the  $^{12}\text{C}(p,\gamma)^{13}\text{N}$  reaction on graphite). To determine the proton efficiency, the resulting average proton current is then compared to the average value of the total current during this time (as measured with a resistive shunt in the outer conductor of the SOL diode).

The striking feature of the double anode configuration is its unidirectionality. Nearly all (>95%) of the protons are emitted in the forward direction. When  $A_1$  and  $A_2$  are interchanged (i.e., the proton source is located at  $A_1$ ), most (> 95%) of the proton current flows only toward the cathode. With a 2- $\mu\text{m}$ -thick  $A_1$  foil (whose thickness is small compared to the 8- $\mu\text{m}$  range of 500-keV protons), no radioactivity from backstreaming protons is detected on the cathode nor on BN targets placed around the cathode. Thus, the unidirectionality of the proton current is evidently due solely to the potential distribution and not to stopping by the aluminized mylar anode.

As a result of its unidirectionality, the efficiency of the double anode configuration is considerably higher than that of an ordinary reflex triode. Proton to total current ratios of  $\geq 50\%$  are obtained with this configuration compared to maximum efficiencies of  $\leq 30\%$  previously observed with reflex triodes under the same conditions. About  $9 \times 10^{14}$  protons per pulse are detected ( $E > 277$  keV), i.e., about twice that generated with ordinary reflex triodes under similar conditions. These results may not represent the maximum efficiency, since a systematic optimization of parameters has not yet been performed.



The performance of the double anode device is characterized by a substantial delay in impedance collapse when compared to a reflex triode with the same anode-cathode spacing. This phenomenon is illustrated in Fig. 2, which shows voltage and current traces for each case.

The anode voltage is initially the same in both the reflex triode and the reflex tetrode. However, about 30 nsec after the initiation of the voltage pulse, the impedance drops sharply in the reflex triode (dashed curves), resulting in a considerably shorter voltage pulse. The total current of the reflex tetrode is about  $1/3$  that of the simple reflex triode. This suggests that the plasma formed at  $A_1$  is not dense enough to provide sufficient numbers of protons to neutralize the electron space charge in the cathode- $A_1$  region. Thus, the cathode emission is substantially reduced.

Framing photography is used to compare plasma formation and propagation in the reflex tetrode configuration to that in a conventional reflex triode (i.e., with polyethylene foil on  $A_1$  or  $A_2$  and the second anode removed). An image converter camera photographs the anode assembly from the side in three 10-nsec exposures on each shot. In Fig. 3, a microdensitometer analysis of a typical set of framing photographs illustrates the operation of the reflex tetrode. Bright areas corresponding to the two anode plasmas and the cathode plasma can be seen. The important feature is that the plasma formed at  $A_1$  (from the aluminized mylar) remains essentially stationary, while the  $A_2$  plasma (formed from the polyethylene) moves downstream.

By incorporating photographs from several shots, it is possible to examine the time history of the plasma expansion. In Fig. 4, data are plotted

for three cases: (a) the reflex tetrode, (b) a reflex triode with polyethylene anode at  $A_2$ , and (c) a reflex triode with polyethylene anode at  $A_1$ . In the reflex triodes, the emitted light is dim, and it is difficult to see the plasma expansion inside the aluminum anode ring, even though a 1-cm-long section of it has been removed to allow photographing between  $A_1$  and  $A_2$ . It is clear from these results that the  $A_1$  plasma expands toward the cathode in the reflex triode case (Fig. 3c), but not in the reflex tetrode configuration. In general, the plasma expansion velocity away from the polyethylene anode is  $\sim 1.7$  cm/ $\mu$ sec.

In a small number of shots, we have investigated the presence of high energy protons in the double anode configuration. Using the  $^{63}\text{Cu}(p,n)^{63}\text{Zn}$  reaction,<sup>11</sup> it has been concluded from the activation induced on stacked copper foil targets that  $\sim 2\text{-}5 \times 10^8$  protons with energy  $\geq 5$  MeV are generated. The presence of these high energy protons suggests a time-dependent potential profile. This aspect of the double anode configuration is evidently similar to that of an ordinary reflex triode, in which we measured similar numbers of 5-6 MeV protons.

In conclusion, a new tetrode configuration has been developed that is characterized by a unidirectional proton beam and high proton generation efficiency.



### References

1. J. Golden, C.A. Kapetanacos, S.J. Marsh and S.J. Stephanakis, Phys. Rev. Lett. 38, 130 (1977).
2. C.A. Kapetanacos, J. Golden and W.M. Black, Phys. Rev. Lett. 37, 1236 (1976).
3. S.J. Stephanakis, D. Mosher, G. Cooperstein, J.R. Boller, J. Golden and S.A. Goldstein, Phys. Rev. Lett. 37, 1543 (1976).
4. S. Humphries, T.J. Lee and R.N. Sudan, Appl. Phys. Lett. 25, 20 (1974);  
M. Greenspan, S. Humphries, Jr., J. Maenchen, and R.N. Sudan, Phys. Rev. Lett. 39, 24 (1977).
5. D.S. Prono, J.W. Shearer and R.J. Briggs, Phys. Rev. Lett. 37, 21 (1976).
6. S.C. Luckhardt and H.H. Fleischmann, Appl. Phys. Lett. 30, 182 (1977).
7. S.A. Goldstein and R. Lee, Phys. Rev. Lett. 35, 1079 (1975).
8. J.M. Creedon, I.D. Smith and D.S. Prono, Phys. Rev. Lett. 35, 911 (1975).
9. T.M. Antonsen, Jr. and E. Ott, Phys. Fluids 19, 52 (1976).
10. J. Golden, C.A. Kapetanacos, S.J. Marsh and S.J. Stephanakis, NRL Report No. 3422, 1976.
11. F.C. Young, J. Golden and C.A. Kapetanacos, Rev. Sci. Instr. 48, 432 (1977).

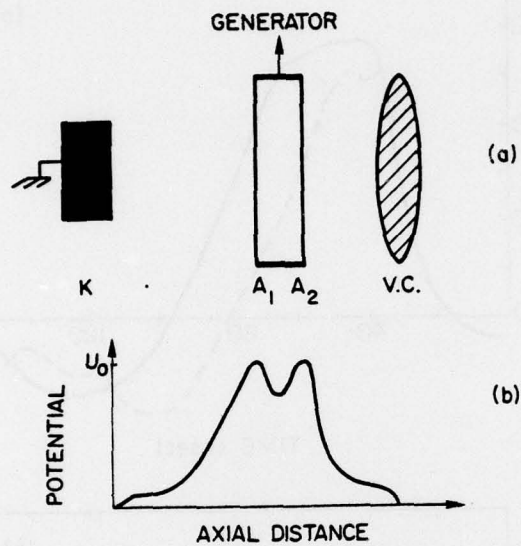


Fig. 1 — (a) Schematic of reflex tetrode, and (b) qualitative electric potential profile of this configuration

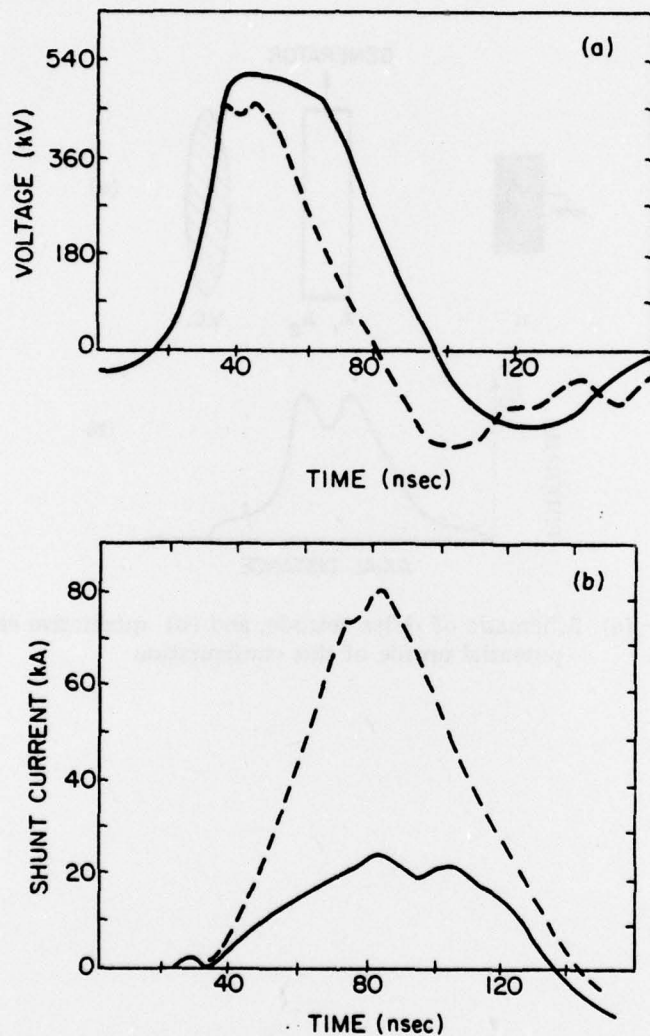


Fig. 2 — (a) Diode voltage traces for the reflex tetrode (solid curve) and reflex triode (dashed curve), and (b) corresponding shunt currents for the two cases. For the reflex tetrode  $A_1-K \approx 1.1\text{cm}$  and  $A_2-K \approx 1.6\text{cm}$  while for the reflex triode  $A-K = 1.6\text{cm}$ .



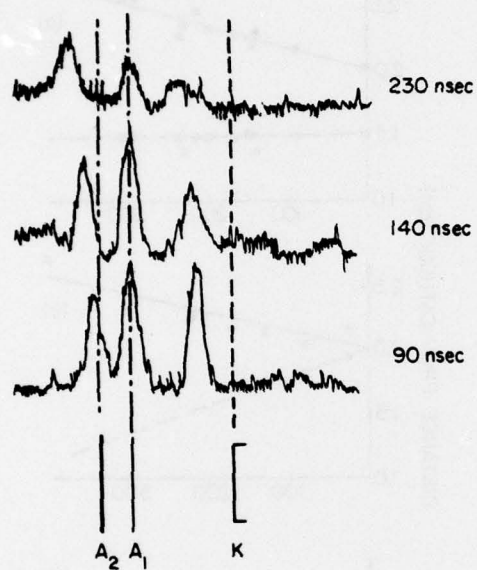


Fig. 3 — Microdensitometer analysis of a set of framing photographs, taken in three 10-nsec exposures at various times after initiation of the voltage pulse, for the reflex tetrode.  $A_1$ -K gap is 1.5cm.

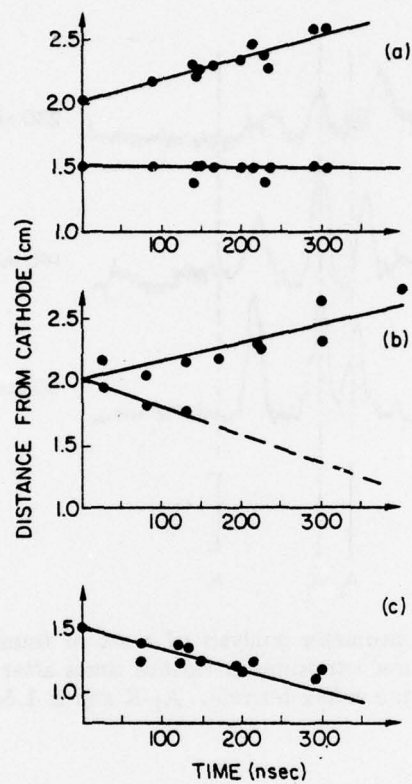


Fig. 4 — Position of anode plasma fronts at various times as determined by framing photography in three configurations: (a) reflex tetrode, (b) reflex triode with polyethylene at  $A_2$ , (c) reflex triode with polyethylene at  $A_1$ .